Low-temperature photoluminescence upconversion in porous Si

D. Kovalev, J. Diener, H. Heckler, G. Polisski, N. Künzner, and F. Koch
Technische Universität München, Physik-Department E16, D-85747 Garching, Germany

Al. L. Efros and M. Rosen
Nanostructure Optics Section, Naval Research Laboratory, Washington, DC 20375
(Received 15 July 1999)

We report efficient low-temperature upconverted photoluminescence (UPL) at resonant excitation of the porous Si photoluminescence band. The UPL has a linear dependence on the excitation intensity, quenches at elevated temperatures, and is absent in strongly oxidized porous Si and oxidized Si nanocrystals. These observations are explained by the resonant excitation of electron-hole pairs spatially separated in neighboring crystals. UPL results from the subsequent excitation of a second pair in the larger of the two crystals and Auger ejection of a carrier into the smaller one, with the larger gap.

A property of nanocrystal assemblies that holds great promise for future applications is their strong nonlinear optical response.[1,2] The coexistence of two electron-hole (e-h) pairs in a nanocrystal leads to Auger photoluminescence (PL) damping, Auger autoionization, and subsequent Auger quenching of the PL in the ionized crystal.[3] These effects have been clearly observed in single CdSe and InAs nanocrystals.[4–6] Porous silicon films are assemblies of silicon nanocrystals and nanowires.[7,8] The very long radiative decay time of their e-h pairs, microseconds to milliseconds,[9] allows nonlinear effects to be especially strong and observable at very low excitation intensity. These lead to PL photodegradation[10] and to the optically induced polarization anisotropy of the PL in porous Si.[11] In this paper we consider another important consequence of Auger autoionization—efficient low-temperature upconversion of the PL.

Upconverted, or anti-Stokes PL (UPL) has been observed in several different inhomogeneous media under resonant optical excitation: in heterostructures,[12–14] sets of quantum wells,[15–17] amorphous Si,[18] fluctuating width quantum wells,[19] and recently, in an ensemble of nanocrystals.[20] In all these experiments the UPL lies within the nonresonant PL spectrum (excited well above the absorption band edge) and obviously originates from the same emitting states as the PL. The additional energy necessary for the UPL can be provided by a phonon bath. In this case, the intensity of the UPL grows with increasing temperature as is seen in Ref. 19. However, when experiment shows the opposite temperature dependence, the additional energy can only come from a second photon excitation[13] or from the nonradiative Auger recombination of a second e-h pair.[12,14,15] These experiments show an almost linear dependence of the UPL intensity on excitation intensity well below the PL saturation limit. This behavior can be explained in terms of a two-step absorption process, and assuming saturation of a long-lived intermediate state.[12,14,15,20] However, the nature of this long-lived state, which strongly depends on the heterostructure type[13,14] and the sample structure,[15] is well understood only for type-II heterostructures.[12]

Our ability to control the size distribution and the surface of the Si nanocrystals in porous Si films together with their long radiative lifetime makes this material an almost ideal system for studying UPL. We show that the long-lived intermediate state characterized in porous Si at low temperatures behaves like a spatially separated e-h pair state with the electron and the hole existing in neighboring nanocrystals. Optical excitation of a second e-h pair in the larger of these nanocrystals leads to the Auger injection of a carrier into the smaller one and subsequent UPL emission. Measured time dependences of the PL and UPL transient behavior indicates that the UPL from the smaller nanocrystals is accompanied by quenching of the PL in the larger ones. This phenomenon is a direct consequence of the process described above.

The UPL in porous Si is observed at resonant excitation of a broad PL band. We performed these experiments over a wide range of excitation energies on sets of hydrogen-passivated and naturally oxidized porous Si samples, and strongly oxidized Si nanocrystals. These samples have nonresonant PL maxima in the range 1.5–2.1 eV. The first two sets of samples were prepared from (100)-oriented p-type c-Si with resistivities $4-6\,\Omega$ cm. Anodization in the dark was carried out in a 50% HF-ethanol solution. To produce the layers with different mean size Si nanocrystals, a change of the HF-ethanol ratio from 3:7 to 2:1 was made. The strongly oxidized Si nanocrystals were prepared either by oxidation of macroporous Si layers made from a heavily boron-doped c-Si with the procedure described in (Ref. 21) [initially containing crystallites with typical sizes 10–20 nm (Ref. 22)] at $T=1000°\mathrm{C}$ for 40 min, or by Si ion implantation in a SiO_2 layer (50 keV at a fluence of 5×10^{16} cm^{-2}) and a subsequent annealing at $T=1100°\mathrm{C}$ for 15 min. A (cw) HeCd (2.8 eV) and Ti-sapphire laser is used to excite the nonresonant and resonant PL, respectively, and a Si charge-coupled device or a fast photomultiplier is employed for detection. To suppress stray light from the exciting chopped cw laser, the entrance slit of the monochromator is blocked by a mechanical shutter when the laser beam illuminates the sample. Thus the light detection is time-delayed: the time interval between mechanical shutting of the laser beam and opening of the monochromator slit is about 20 μs and much faster than the characteristic decay times of both the PL and the UPL (see Fig. 2). This technique provides nearly complete laser light

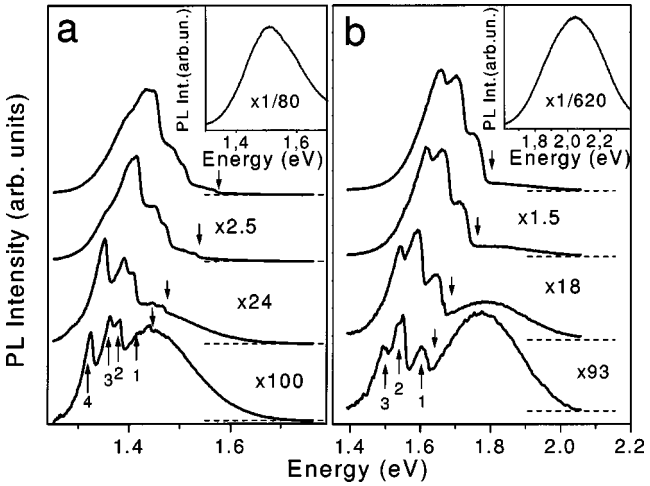

FIG. 1. Resonantly excited PL spectra of two porous silicon samples having different average nanocrystal sizes. (a) Naturally oxidized. (b) Hydrogen passivated. Excitation energies are indicated by down arrows, $T=4.2$ K, $I_{ex}=1$ W/cm^2. Up arrows label the features of the PL associated with no-phonon (NP) and momentum-conserving phonon-assisted transitions. (a) 1:TA-, 2: TO-, 3:TA+TO-, and 4:2TO-phonon-assisted precesses, respectively. (b) 1:NP, 2:TO-, 3:2TO-. Nonresonantly excited PL spectra ($E_{ex}=2.8$ eV) are shown in the insets.

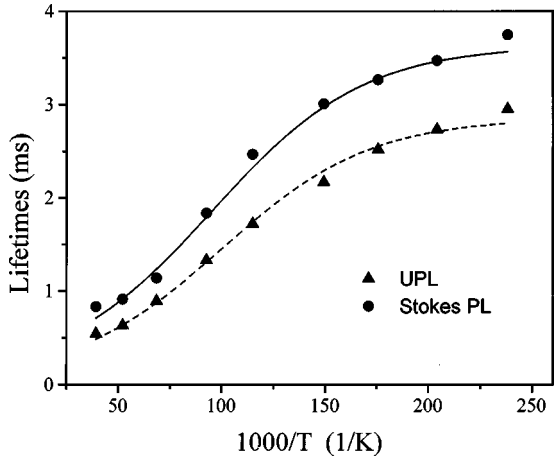

FIG. 2. The temperature dependence of the Stokes PL (circles) and UPL (triangles) lifetime. Solid and dashed lines are fits according to the procedure described in Ref. 23.

suppression and collection of the emitted light from the sample. All PL spectra are normalized to correct for the sensitivity of the optical system.

Figure 1 shows typical low-temperature resonant PL spectra (a) naturally oxidized (kept for one year under ambient conditions) and (b) hydrogen-passivated porous Si samples excited on the low-energy side of the nonresonant emission band (shown in the insets). The Stokes PL consists of a set of peaks assigned to transitions involving no-phonon and 1TA, 2TA, 1TO, TO+TA, and 2TO momentum-conserving phonons in the absorption-emission cycle.[23,24] The spectra also show intense upconverted emission which grows progressively relative to the Stokes PL with decreasing excitation energy. The efficiency of the upconversion is, contrary to the references cited above, very large: at the lowest excitation energy used, the intensity of the UPL reaches the intensity of the Stokes PL.

One should mention that while the intensity of the UPL reaches the intensity of the Stokes PL at the lowest energy of the exciting light, the intensity of these features is down by two orders of magnitude relative to the resonant PL observed at the highest excitation energy used. In addition, a similar difference exists for the PL quantum yield for the resonant excitation[25] relative to that for nonresonant excitation; resonant excitation is an extremely inefficient process. However, as is seen from PL hole burning measurements,[10] the occurrence of phonon replicas of the PL is a general feature of the light emission from porous Si even under efficient nonresonant excitation; thus the inefficiency of the resonant excitation is a result of the low density of intrinsic electronic states inside Si nanocrystals in the vicinity of the excitation energy.

At this point one must ask two questions concerning the nature of the anti-Stokes PL. Is the source of the UPL identical to that responsible for the Stokes part of the spectra, and what is the mechanism for the energy gain? Among all possible scenarios of energy gain, a few can be ruled out easily. At experimental temperatures ~ 4 K, the thermal energy available for upconversion from the phonon bath is much too small to explain the spectral extension of the UPL spectra of up to a few hundreds of meV. A simultaneous absorption of two exciting photons involving extremely short-lived virtual states is impossible as well; it requires much higher excitation intensities, of order MW/cm^2-GW/cm^2, than those used in our experiments (the UPL band still can be observed at intensities even less than 0.1 W/cm^2).

The source of the UPL can be identified by a comparison of the behavior of the lifetime of the Stokes and anti-Stokes PL. For the conventional PL of Si nanocrystals, the lifetime is determined by the thermal equilibrium between the short-lived spin-singlet and the long-lived spin-triplet luminescing exciton states, with lifetimes $\tau_{singlet}\sim\mu$s and $\tau_{triplet}\sim$ms, respectively.[23] As shown in Fig. 2, the lifetime of the UPL exactly follows the two-level statistics of the conventional PL and is in quantitative agreement with Ref. 23. This suggests that excitons confined in Si nanocrystals are responsible for both the PL and UPL emission. As a result, the shape of the UPL band is also determined by the size distribution of the Si nanocrystals, but its peak is $\sim 0.1-0.2$ eV lower in energy than the nonresonantly excited PL peak [see Fig. 1(a) and Fig. 1(b)].

It takes at least two exciting photons to generate the UPL in our case, and thus we might expect the intensity of the UPL to scale nonlinearly with the excitation intensity. However, Fig. 3 shows that the UPL intensity is a linear function of the excitation intensities over a wide range of intensities (and only at $I_{ex}<10^{-1}$ W/cm^2 does it become weakly superlinear). The intensity of the Stokes PL, measured at the energy of the 2TO-phonon peak, is a linear function of the excitation intensity up to ~ 10 W/cm^2; above this, the intensity of both the Stokes PL and the UPL begins to saturate. At this point one should mention that destabilization of Si nanocrystal surface chemistry at high excitation power has been reported by different groups, and that this leads to irreversible PL degradation (for a detailed discussion, see Ref. 26). Most of these measurements were done at room temperature and ambient conditions. In addition, high excitation energies were used, so that the light was efficiently absorbed and the

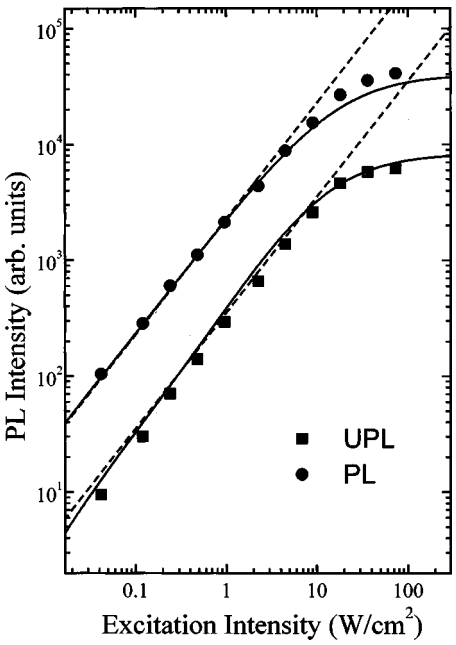

FIG. 3. Excitation intensity dependence of the PL measured at the 2TO peak energy position (circles) and UPL ($E_{det}=1.5$ eV, squares). $T=4.2$ K, $E_{ex}=1.483$ eV. The solid lines are steady-state solutions of the rate equations in the text. The dashed lines are indicated to show a linear dependence on the excitation intensity.

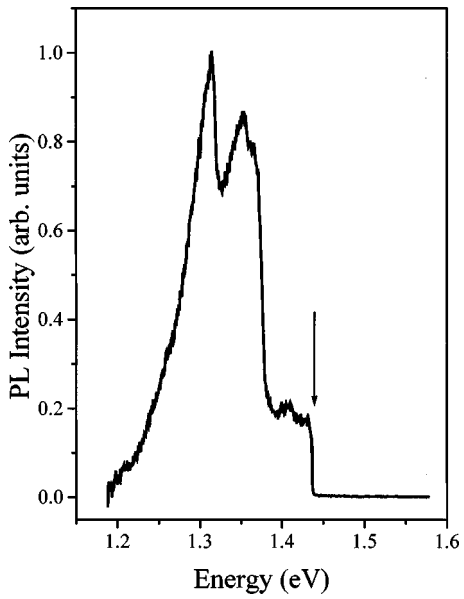

FIG. 4. Resonantly excited PL from Si nanocrystals having a thick oxide shell, $T=4.2$ K, $I_{ex}=1$ W/cm^2. The excitation energy is indicated by the arrow.

power density was very high. Our measurements, however, have been performed at liquid He temperatures, which assures efficient cooling of our samples. Since the PL and UPL power laws have been measured on a seconds time scale, we did not detect any irreversible PL degradation phenomena at even an order of magnitude higher excitation intensity with low-energy light. The linear dependence of the UPL intensity suggests that there is an intermediate long-lived *e-h* pair state in part of the process giving rise to the UPL. The long decay time of these states allows them all to be occupied at very low excitation intensities. The UPL is due to the absorption, now, of a second photon, which provides the excess energy. In order to explain the observed linear behavior, the lifetime of the intermediate state has to be significantly longer than the exciton lifetime in Si nanocrystals [on the order of ms (Ref. 23)].

This long-lived intermediate state can only be an *e-h* pair with a very small overlap integral between localized electron and hole states. The overlap is small if one of the particles is localized at the crystal surface (in this case the first photon excites band and midgap states) or if they are in two neighboring crystallites (in this case the first photon creates the two band states in different crystals). To clarify this point, we have performed a set of independent experiments. The first indication that midgap states are not involved in the UPL excitation mechanism comes from similarities of lifetimes of the PL and UPL at low temperatures. If the second absorption event occurs through a midgap state, the final excited state giving rise to UPL has to be considered as having an unphysically long lifetime, in the millisecond range. A second indication comes from hydrogen effusion experiments. As it was well documented in Ref. 27, removing the passivating hydrogen from the surface of the crystallites creates a large number of such midgap states (dangling bonds) which act as nonradiative defects. This lowers the external PL quantum efficiency by a factor on the order of 100; we find that neither the relative intensities nor the spectral shape of the PL and UPL are changed. If midgap states were the intermediate states in the upconversion process, one would expect a relative increase of the UPL with respect to the Stokes PL. One might consider that hydrogen is an important component of the photoluminescent emitter. However, the well-pronounced momentum-conserving phonon replicas of the Stokes PL give evidence that the Si crystalline core is responsible for the light emission.

The role of charge separation can be also studied by using nanocrystals isolated by high potential barriers. Figure 4 shows the resonant PL spectrum for a system of Si nanocrystals surrounded by a thick SiO_2 shell which prevents any carrier transfer between the crystallites. These nanocrystals have been produced by Si ion implantation in a SiO_2 layer, which ensures the presence of such a shell. While the same combination of momentum-conserving phonon peaks is observed as in Fig. 1, UPL is completely absent. This is true for all the excitation energies we used. This observation implies that carrier transfer between nanocrystals plays a crucial role in the upconversion process. There should be no significant difference between an assembly of isolated nanocrystals and a nanocrystal network if the midgap states inside of a single nanocrystal were responsible for the UPL emission.

The polarization of the UPL in porous silicon can reveal information about the excitation mechanisms of the UPL and Stokes PL. The polarization properties of porous Si PL are determined by the anisotropic shapes of randomly oriented Si crystals.[28] Linearly polarized light selectively excites those crystals whose largest dimension is parallel to the vector polarization of the exciting light. This is because inside the nanocrystal the resultant depolarization decreases the component of the electric field along that axis less than it does the other components. The light subsequently emitted by these crystals is also predominantly polarized along the

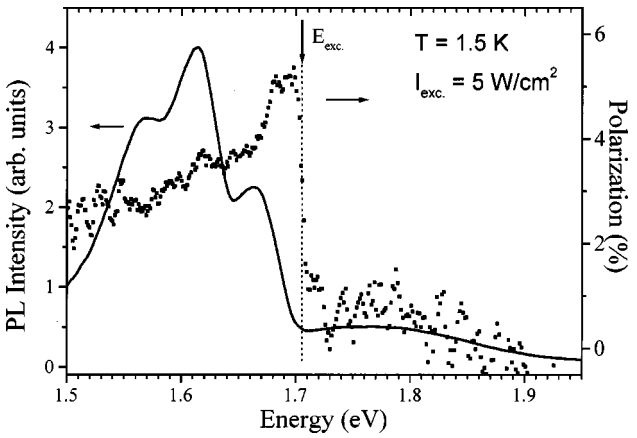

FIG. 5. Resonant PL and UPL spectrum from porous Si (solid line) and the luminescence polarization (solid squares). Note the sharp decreases of the polarization above the energy of the exciting light.

same direction. This results in a strong polarization memory effect that is determined by the crystal shapes only (one can find a review of this effect in Ref. 29).

Figure 5 shows both the PL spectrum from the naturally oxidized sample excited by linearly polarized light, and its polarization. The relative strength of the UPL was kept low so as not to affect the degree of polarization of the Stokes PL. The linear polarization memory effect is defined as the ratio $\rho=[(I_{\parallel}-I_{\perp})/(I_{\parallel}+I_{\perp})]\times 100\%$, where $I_{\parallel}(I_{\perp})$ is the intensity of the PL polarized parallel (perpendicular) to the direction of the electric field of the exciting light. One can see that at energies below the excitation the PL is polarized. Furthermore, the polarization decreases towards lower detection energies, in agreement with Ref. 30. This reflects the polarization selective absorption-emission cycle occurring in the same nanocrystal.[28,30] In contrast, the UPL is nearly unpolarized with a very sharp transition at the excitation energy. The absence of polarization of the UPL suggests that the emitting nanocrystal is different from the excited one as would be expected from a model that assumes a spatial separation of the electron and hole in separate crystals. If a sequential two-photon absorption within a single crystallite were responsible for the upconversion, the UPL would also show the polarization memory effect.

Taking all this into account suggests the model of UPL in porous Si that is shown schematically in Fig. 6. Si nanocrystals in hydrogenated porous Si samples are not separated by the high potential barrier that exists in strongly oxidized samples. This allows direct excitation of coupled neighboring crystals, with the excited carriers localized in different crystals. These states have a very long decay time. The generation of a second *e-h* pair in the larger of the two crystals then results in the Auger ejection of the remaining carrier into the smaller neighbor (which has a larger gap). Subsequent recombination of the *e-h* pair in that crystal gives the UPL. A system of rate equations describing the occupation of these coupled nanocrystals, from which we can obtain the UPL at excitation frequency, ω, can be written

$$\dot{N}_0=-WN_0-W_{\rm in}N_0+\frac{N_1}{\tau_r}+\frac{N_s}{\tau_{\rm in}}+\frac{N_u}{\tau_r},$$

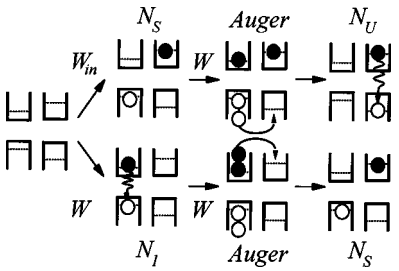

FIG. 6. A schema of the coupled dot model for generation of the UPL in hydrogenated porous Si. W and $W_{\rm in}$ are generation rates for the different excitation paths in a system of coupled nanocrystals. $N_{1,U,S}$ are the concentrations of crystallites having specific occupation scenarios indicated in the text. The word open ''Auger'' labels an intermediate Auger event.

$$\dot{N}_1=WN_0-WN_1-\frac{N_1}{\tau_r},$$

$$\dot{N}_s=W_{\rm in}N_0-\frac{N_s}{\tau_{\rm in}}-WN_s+WN_1, \tag{1}$$

$$\dot{N}_u=WN_s-\frac{N_u}{\tau_r},$$

where $N_{0,1,s,u}$ are, respectively, the concentration of neighboring crystals with zero *e-h* pairs in both of the coupled crystals, one *e-h* pair in the larger crystal (smaller absorption edge), one electron and one hole occupying separate crystals, and one *e-h* pair in the smaller crystal (large energy gap); $N_0+N_1+N_s+N_u=N(\omega)$, $N(\omega)$ is the concentration of coupled pairs of crystals, one of which has an energy gap greater than the excitation energy, $\hbar\omega$, and the other whose energy gap is smaller than $\hbar\omega$, τ_r is the intrinsic exciton radiative lifetime in a nanocrystal, $\tau_{\rm in}$ is the recombination time of a separated *e-h* pair, $W=\sigma I_{\rm ex}/\hbar\omega$ and $W_{\rm in}=\sigma_{\rm in}I_{\rm ex}/\hbar\omega$, where $\sigma(\omega)$ and $\sigma_{\rm in}(\omega)$ are, respectively, the absorption cross section for the direct excitation of the larger crystal and for a spatially separated *e-h* pair, and $I_{\rm ex}$ is the intensity of the exciting light.

Equation (1) assumes that all Auger processes are much faster than typical radiative transition times (a very good approximation for Si nanocrystals.[31]) This means that the excitation of a second *e-h* pair in a crystal which already contains a pair leads instantaneously to the ionization of the crystal and to a spatially separated *e-h* state (this process is described by the term WN_1). Excitation of an *e-h* pair in an already ionized crystal leads to the generation of an *e-h* pair in the nanocrystals with a larger energy gap (this process is described by the term WN_s). We also assume that the barrier height for one of the carriers (a hole in our scheme) is significantly larger than for the second one. As a result, a hole cannot be ejected into the smaller crystal unless there is already an electron there which decreases this effective barrier height.

The steady-state solution of the kinetic state-filling equations [Eq. (1)] gives the following intensity dependence of the UPL:

$$I_u \sim \frac{N_u}{\tau_r} = \frac{WS_{\text{in}}[\alpha+(1+\alpha)W\tau_r]N(\omega)}{1+2W\tau_r+S_{\text{in}}[\alpha+(1+\alpha)W\tau_r](1+W\tau_r)}, \quad (2)$$

where $\alpha = W_{\text{in}}/W$ and $S_{\text{in}} = \tau_{\text{in}}W/(1+\tau_{\text{in}}W)$. The UPL intensity is proportional to τ_{in} and therefore the existence of the long-lived intermediate state is essential. One can see that at very low excitation intensity, below the saturation region of the intermediate state ($W\tau_{\text{in}} < 1$), the UPL is a superlinear function of the excitation intensity. In the saturation region of the intermediate state ($W\tau_{\text{in}} \gg 1$), it behaves linearly. Deviation from the linear regime occurs again at the Auger saturation condition for both the UPL and Stokes PL ($W\tau_r > 1$, double occupation of nanocrystals by two *e*-*h* pairs). The calculated dependence is shown in Fig. 3. The result of similar considerations for the intensity of the Stokes PL for isolated crystals is also shown in Fig. 3. The following experimental values for porous Si were used in these calculations: $\sigma = 1.1\times10^{-18}$ cm^2 (derived from the PL Auger saturation, see Ref. 11) and the intrinsic exciton radiative recombination time $\tau_r = 3$ ms. The fitting parameters $\alpha = 0.3$ and $\tau_{\text{in}} = 3$ s give the best description of our data for $E_{\text{ex}} = 1.483$ eV.

We find strong further support for our model in the study of the temporal response of the UPL and the Stokes PL. Our model predicts that, at a low enough excitation intensity, after the beginning of the cw optical excitation, a specific transient behavior occurs before a steady-state condition of charge separation and indirect recombination is achieved. The slow build up of space-separated *e*-*h* pairs in neighboring crystals leads to a time-dependent growth of the UPL. This is accompanied by an Auger suppression of the Stokes PL from the larger crystals of the neighbor pair (due to their being charged). This transient process is expected to be faster at higher light intensities. Figure 7 shows the temporal response of the spectrally integrated UPL (a) and Stokes PL (b) for an abrupt steplike onset of the exciting laser at time zero. The selection of the spectral range was done using long and high-pass optical filters in front of a photomultiplier tube. The beam of a cw Ti-sapphire laser was opened within 20 microseconds at time zero by a mechanical shutter. The kinetics of the Stokes PL have been measured at a somewhat higher excitation energy than that of the UPL to avoid spectral overlap of two PL bands. At low excitation energy, the excitation intensity is chosen higher in order to maintain a reasonable signal-to-noise ratio. These experiments were performed at $T = 4.2$ K, after initial heating of the samples to $T = 300$ K, to assure that any previously charged nanocrystals are neutralized by thermally induced charged-carrier transport. The UPL rises with time from zero to a steady-state intensity. The rise time is excitation intensity dependent and is shorter at higher intensity. In contrast, the Stokes PL intensity decreases with time until it reaches a constant value, which is about 90% of its initial strength (for clarity we have substracted the intensity of the Stokes PL observed after the transient process under cw excitation conditions). The Stokes PL decay time and rise time for the UPL depend the same way on the intensity. In Fig. 7 we show the transient processes calculated using the time-dependent solution of Eq. (1) with the same parameters used to describe the intensity dependence.

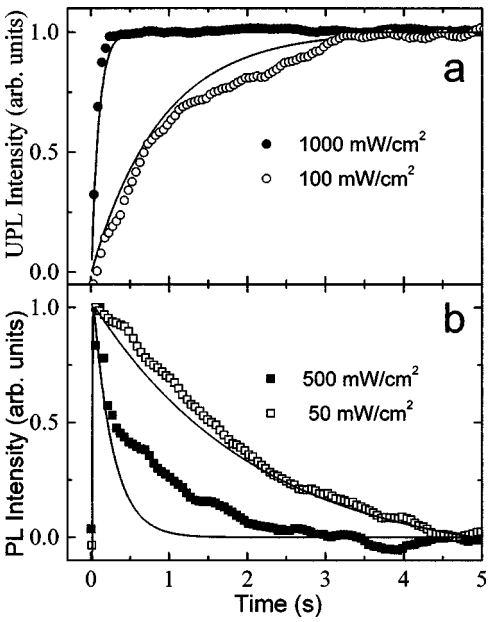

FIG. 7. Temporal dependence of the UPL [(a), circles, $E_{\text{ex}} = 1.48$ eV] and Stokes PL [(b), squares, $E_{\text{ex}} = 1.57$ eV]; the CW PL level has been substracted. $T = 4.2$ K. The excitation intensities are indicated. Solid lines are solutions of the time-dependent rate equations in the text.

The existence of long-lived spatially separated charges is crucial for our model of the UPL. To describe the observed UPL intensity dependence, one has to assume that the lifetime of the intermediate state is on the order of seconds. Experimental evidence for such states comes from the observation of an extremely long-lived component of the PL (see Fig. 8). This fluorescence was measured at $T = 1.5$ K after initial cw illumination of the sample (immersed in superfluid He ambient to avoid heating during illumination) by a high-energy 2.54 eV Ar-ion beam laser for 5 min. The excitation intensity $I_{\text{ex}} = 10$ W/cm^2 was chosen to be many orders of magnitude less than that used for the two-photon excitation. This illumination creates spatially separated *e*-*h* pairs which recombine slowly after switching off the excitation source. The spectrally integrated FL response, integrated over a 10 s time window, has been measured at 10 s intervals. The decay

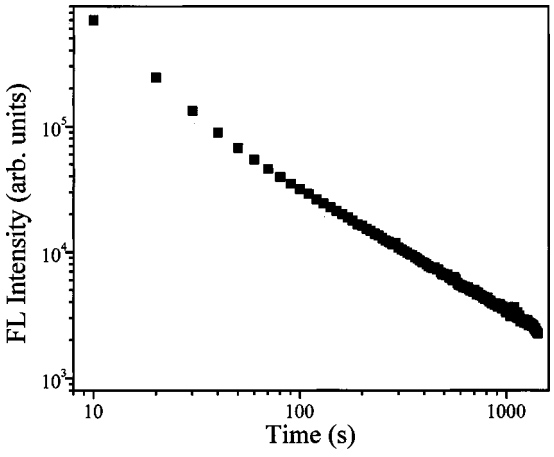

FIG. 8. The decay curve of the spectrally integrated long-lived fluorescence. Signal integration time is 10 s. $T = 1.5$ K.

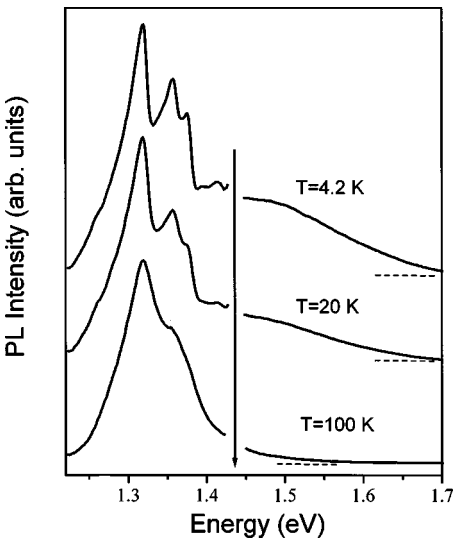

FIG. 9. Resonant PL spectra from a hydrogen-passivated sample at different temperatures. $I_{ex}=1$ W/cm^2. The excitation energy is indicated by the arrow.

is strongly nonexponential and it varies over three decades from seconds to 10 min. However, the main contribution to the quantum yield of the FL comes from recombination lifetimes on the order of seconds. This is consistent with the value we used for τ_{in}, and with the cw PL and UPL transient times shown in Fig. 7. The FL decay behavior, moreover, is strongly temperature-dependent. This shows that nonexponential decay of the FL may be connected with a distribution of barrier heights which the carrier must overcome before recombination can occur. The higher the temperature, the larger is the amplitude of the FL and the shorter the decay time. Exact information on the time-integrated FL intensity is not experimentally available since the heating of the sample to elevated temperature takes place on a 10 sec scale. During the heating process the amplitude of the FL is rising. However, according to our measurements the FL intensity (integrated over the heating to 20 K and with stabilized temperature time domains) is of the same order as at low temperature (1.5 K). We believe that increased temperature stimulates transport between the crystallites and thus accelerates the recombination of the separated *e-h* pairs. It is necessary to mention that, in fact, the value of $\tau_{in}=3$ s should be considered as an average value for the spectrally integrated PL and UPL seen in Figs. 7 and 8. However, it gives a satisfactory fit for all experiments described above.

As seen in Fig. 9, temperature-stimulated carrier transport also results in a strong dependence of the UPL intensity on the ambient temperature. While the integrated intensity of the Stokes PL remains almost constant with rising temperature (the smearing of the exciton peaks is due to interaction with acoustical phonons), the UPL intensity vanishes rapidly. At 100 K the UPL band disappears completely (the weak anti-Stokes tail seen is due to thermal smearing of the Stokes PL).

In Fig. 1 we saw that the relative strength of Stokes and anti-Stokes PL also depends strongly on the position of the excitation energy inside the nonresonantly excited luminescence band. The UPL intensity grows relative to the intensity of the Stokes PL with decreasing excitation energy, and becomes comparable to it at the red edge of the porous Si PL band. This implies two things. First, that the concentration of coupled crystals excited at the red edge of the PL line, $N(\omega)$, is greater than that of isolated crystals. This is consistent with the fact that, on the red edge, any crystallite has a higher probability of pairing with a smaller neighbor (a possible emitter for high-energy UPL), and the largest crystallite is always surrounded by smaller ones.

It also implies that, for very low excitation energy, $W_{in} \sim W$, which can be directly seen from the comparable amplitudes of the PL and UPL bands (this also justifies the value of $\alpha=0.3$ for the calculated UPL power dependence). This unexpected result may be connected with the suppression of phonon-assisted direct excitation of the largest nanocrystals where energy conservation allows only zero phonon optical absorption (under resonant excitation). The probability of direct zero phonon excitation of a single nanocrystal and of space-indirect excitation of coupled crystals can be comparable, because, in both tunneling and confinement, the barrier leads to breakdown of the *k*-conservation rule necessary for indirect phononless transitions.

Despite the simplicity of our model, it describes all our UPL experimental results very well. The crucial feature in the model is the existence of a long-lived spatially separated *e-h* pair state. The lifetime of this state, derived from the UPL power dependence, is of the order of seconds and is in good agreement with both the specific transient behavior of the PL and UPL bands and the extremely long-lived fluorescence whose characteristic transient times have a similar value. The particular properties of porous Si allow us to identify the particular nature of this intermediate state and the mechanism of the secondary excitation. This can be difficult in other inhomogeneous systems which exhibit UPL. We believe, however, that, in a general sense, this model shares the common feature of the luminescence upconversion phenomena in all these systems. That is the existence of a long-lived spatially separated intermediate *e-h* pair state, which can accumulate carriers for either subsequent Auger or direct optical excitation into high-energy states which are responsible for the UPL.

This work was supported by the Office of Naval Research.

[1] S. Schmitt-Rink, D.A.B. Miller, and D.C. Chemla, Phys. Rev. B **35**, 8113 (1987).

[2] P. Horan and W. Blau, Phase Transit. **24-26**, 605 (1990).

[3] D.I. Chepic, Al.L. Efros, A.I. Ekimov, V.A. Kharchenko, I.A. Kudriavtsev, and T.V. Yazeva, J. Lumin. **47**, 113 (1990).

[4] M. Nirmal, B.O. Dabboussi, M.G. Bawendi, J.J. Macklin, J.K. Trautmann, T.D. Harris, and L.E. Brus, Nature (London) **383**, 802 (1996).

[5] S. Empedocles, D.J. Norris, and M.G. Bawendi, Phys. Rev. Lett. **77**, 3873 (1996).

[6] U. Banin, M. Bruchez, J.C. Lee, A.P. Alivisatos, T.J. Ha, S. Weiss and D.S. Chemla, J. Chem. Phys. (to be published).
[7] L.T. Canham, Appl. Phys. Lett. **57**, 1046 (1990).
[8] L.E. Brus, in *Light Emission in Silicon*, edited by D.J. Lockwood, Semiconductor and Semimetals (Academic Press, New York, 1996).
[9] J.C. Vial, A. Bsiesy, F. Gaspard, R. Herino, M. Ligeon, F. Muller, R. Romestain, and R.M. MacFarlane, Phys. Rev. B **45**, 14 171 (1992).
[10] D. Kovalev, H. Heckler, B. Averboukh, M. Ben-Chorin, M. Schwartzkopff, and F. Koch, Phys. Rev. B **57**, 3741 (1998).
[11] D. Kovalev, B. Averboukh, M. Ben-Chorin, F. Koch, Al.L. Efros, and M. Rosen, Phys. Rev. Lett. **77**, 2089 (1996); Al.L Efros, M. Rosen, B. Averboukh, D. Kovalev, M. Ben-Chorin, and F. Koch, Phys. Rev. B **56**, 3875 (1997).
[12] W. Seidel, A. Titkov, J.P. Andre, P. Voisin, and M. Voos, Phys. Rev. Lett. **73**, 2356 (1994).
[13] J. Zeman, G. Martinez, P.Y. Yu, and K. Uchida, Phys. Rev. B **55**, R13 428 (1997).
[14] Y-H. Cho, D.S. Kim, B-D. Choe, H. Lim, J.I. Lee, and D. Kim, Phys. Rev. B **56**, R4375 (1997).
[15] R. Hellmann, A. Euteneuer, S.G. Hense, J. Feldman, P. Thomas, E.O. Göbel, D.R. Yakovlev, A. Waag, and G. Landwehr, Phys. Rev. B **51**, R18 053 (1995).
[16] H. Cheong, B. Fluegel, M.C. Hanna, and A. Mascarenhas, Phys. Rev. B **58**, R4254 (1998).
[17] F.A.J.M. Driessen, H.M. Cheong, A. Mascarenhas, S.K. Deb, P.R. Hageman, G.J. Bauhuis, and L.J. Giling, Phys. Rev. B **54**, R5263 (1996).
[18] X. Yin, J.M. Viner, S.Q. Gu, M.E. Raikh, and P.C. Taylor, Phys. Rev. B **49**, R5073 (1994).
[19] L. Schrottke, H.T. Grath, and K. Fujiwara, Phys. Rev. B **56**, R15 553 (1997).
[20] E. Poles, D.C. Selmarten, O.I. Micic, and A.J. Nozik, Appl. Phys. Lett. **75** 971 (1999).
[21] G. Polisski, H. Heckler, D. Kovalev, and F. Koch, Appl. Phys. Lett. **73**, 1107 (1998).
[22] A.G. Cullis and L.T. Canham, Nature (London) **353**, 335 (1991).
[23] P.D.J. Calcott, K.J. Nash, L.T. Canham, M.J. Kane, and D. Brumhead, J. Phys.: Condens. Matter **5**, L91 (1993).
[24] D. Kovalev, H. Heckler, M. Ben-Chorin, G. Polisski, M. Schwartzkopff, and F. Koch, Phys. Rev. Lett. **81**, 2803 (1998).
[25] M. Rosenbauer, S. Finkbeiner, E. Bustarret, J. Weber, and M. Stutzmann, Phys. Rev. B **51**, 10 539 (1995).
[26] A.G. Cullis, L.T. Canham, and P.D.J. Calcott, J. Appl. Phys. **82**, 909 (1997).
[27] V. Petrova-Koch, T. Muschik, A. Kux, B.K. Meyer, F. Koch, and V. Lehmann, Appl. Phys. Lett. **61**, 943 (1992).
[28] D. Kovalev, M. Ben-Chorin, J. Diener, F. Koch, Al.L. Efros, M. Rosen, N.A. Gippius, and S.G. Tikhodeev, Appl. Phys. Lett. **67**, 1585 (1995).
[29] Al.L. Efros, M. Rosen, B. Averboukh, D. Kovalev, M. Ben-Chorin, and F. Koch, Phys. Rev. B **56**, 3875 (1997).
[30] D. Kovalev, M. Ben-Chorin, J. Diener, B. Averboukh, G. Polisski, and F. Koch, Phys. Rev. Lett. **79**, 119 (1997).
[31] C. Delerue, M. Lannoo, G. Allan, E. Martin, I. Mihalcescu, J.C. Vial, R. Romestain, F. Muller, and A. Bsiesy, Phys. Rev. Lett. **75**, 2228 (1995).